Numerical modeling assisting in surgical treatment of total anomalous pulmonary venous connection in children

Jie Jin ![ORCID],[1] Kaiyun Gu,[2] Jiawei Liang,[3] Jing Yu ![ORCID],[4] Xiangming Fan[1]

[1]Department of Cardiac Surgery, Children's Hospital, Zhejiang University School of Medicine, Hangzhou, China
[2]National Clinical Research Center for Child Health, Children's Hospital, Zhejiang University School of Medicine, Hangzhou, China
[3]Department of Radiology, Children's Hospital, Zhejiang University School of Medicine, Hangzhou, China
[4]Department of Ultrasonography, Children's Hospital, Zhejiang University School of Medicine, Hangzhou, China

Correspondence to
Dr Xiangming Fan;
fanxiangming@zju.edu.cn

ABSTRACT

Objective To develop a model using patient-specific computational fluid dynamics (CFD) to predict the required anastomotic size for total anomalous pulmonary venous connection (TAPVC) surgery and to forecast surgical outcomes.

Methods Based on clinical data from patients, a CFD model was used to simulate the anastomosis between pulmonary venous confluence and the left atrium. Blood flow velocity, wall shear stress, power loss, and pressure were calculated using numerical algorithms within the model. Various sizes of anastomosis were applied during the simulation. The energy dissipation at the anastomosis was computed from the results and compared with real-world data.

Results As the simulated anastomotic size increased, blood flow velocity, pulmonary venous pressure, and energy loss decreased. However, when the anastomotic size exceeded 18 mm, the efficiency of energy conversion no longer improved. The realistic and simulated velocities matched well for anastomosis sizes ranging from 15 to 20 mm.

Conclusion The model can assist surgeons in preoperative planning for determining the anastomotic size in TAPVC surgical treatment.

WHAT IS ALREADY KNOWN ON THIS TOPIC

⇒ The size of anastomosis strongly affects the outcomes of surgical treatment for total anomalous pulmonary venous connection (TAPVC).

WHAT THIS STUDY ADDS

⇒ Our study developed a model that can predict the optimal size of anastomosis for surgical treatment using computational fluid dynamics based on patient-specific data.

HOW THIS STUDY MIGHT AFFECT RESEARCH, PRACTICE OR POLICY

⇒ The model can assist surgeons in planning the anastomosis for TAPVC surgeries.

INTRODUCTION

Total anomalous pulmonary venous connection (TAPVC) is a complex cardiac malformation with low incidence. In TAPVC, all pulmonary veins (PVs) remain connected to systemic veins or are abnormally connected to the right atrium.[1] Despite advancements in surgical techniques and preoperative/ postoperative care, surgical correction of TAPVC has remained challenging over the past decades. The main complication for TAPVC patients is postoperative PV obstruction (PVO), which is also the primary reason for reoperation and a critical factor affecting long-term survival.[2 3] The recurrence of PVO is related to the proliferation of endothelial fibroblasts, primary PV stenosis,[4] and the size of the anastomosis during surgery. Thus, surgeons tend to make the anastomosis as large as possible.[5 6] However, the optimal size of the anastomosis for TAPVC patients preoperatively remains unclear.

To the best of our knowledge, no studies have addressed the prediction of the size of anastomosis for TAPVC patients preoperatively. Additionally, establishing animal models for TAPVC proves to be challenging. Given the high risk and difficulty associated with reoperations in TAPVC patients, designing a prospective research study on this issue would pose ethical concerns. Consequently, conducting research in this area remains challenging.

Computational fluid dynamics (CFD) is a technique that uses algorithms to simulate fluids and analyze fluid dynamics processes. Previous studies have demonstrated the potential of CFD in hemodynamic research, enabling the creation of numerical models of the cardiovascular system. CFD can be used in investigating both adult acquired heart diseases[7–9] and congenital heart diseases.[10–12] In our previous study,[13] we established a CFD model of TAPVC, specifically simulating the anastomosis between the pulmonary common vein (CV) and the left atrium (LA). This model calculates physical parameters, such as blood flow velocity, pressure distribution, wall shear stress (WSS) of vessels, and energy loss. Our study highlights a new surgical method
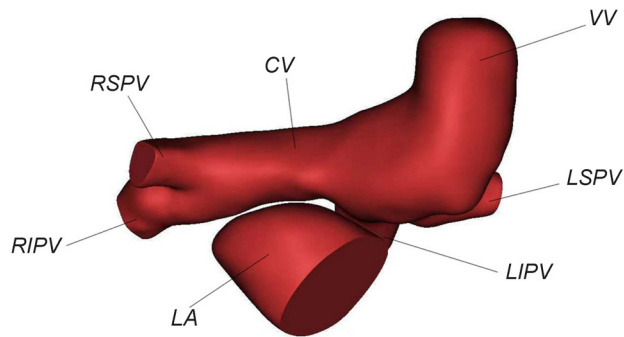
Figure 1 Original three-dimensional geometry, this study includes two components: left atrium and pulmonary veins. CV, common vein; LA, left atrium; LIPV, left inferior pulmonary vein; LSPV, left superior pulmonary vein; RIPV, right inferior pulmonary vein; RSPV, right superior pulmonary vein; VV, vertical vein.

using this CFD model that may offer advantages over traditional approaches in the treatment of TAPVC.

In this study, we used our previous model to simulate surgical outcomes and physical parameters using an array of anastomosis sizes. The geometry of the model is based on preoperative patient-specific imaging data. It is well-established that larger anastomoses typically yield better surgical outcomes. Here, we designed incremental variations in anastomosis sizes for specific patients.

METHODS
Patient and public involvement
Patients or the public were not involved in the design, conduct, reporting or dissemination plans of our research.

Clinic data and geometry building
The three-dimensional (3D) model of TAPVC was constructed based on computer tomography angiography images from patient-specific sources and summarized data from references,[14] including the PV, LA, CV, and part of the vertical vein (figure 1). It was constructed in the computer aided design software of SolidWorks.

In this study, we used clinical data from a 6-year-old boy in our department who was diagnosed with supracardiac type TAPVC accompanied by an atrial septal defect. The child weighed 16.4 kg when enrolled in our center.

In order to evaluate and predict the optimal anastomosis size for surgical treatment of TAPVC, incremental anastomosis sizes were designed to connect the common PV and the LA. The anastomosis was window shaped as described in our previous study.[13] Ten incremental sizes of anastomosis were ranged from 5.5 mm to 28.0 mm, as shown in figure 2. These sizes correspond to the length of incisions which were made by surgeons during surgery.

These 3D models were reconstructed using SolidWorks for further processing. The mesh was generated with HyperMesh software, and the density was increased in regions of interest. The optimal mesh size was determined by performing a mesh independence analysis. The element size on the wall was ranged from 0.2 to 0.8 mm. Additionally, a mesh in the boundary layer was created with the following boundaries: the thickness of the first layer was 0.07 mm, the growth ratio was 1.1 and the number of mesh layers was five.

Materials and boundary conditions
The left atrial wall and blood vessels are assumed to be rigid and non-slip. It is assumed that blood is an incompressible Newtonian fluid with a density of 1050 kg/m^3 and a viscosity of 0.0035 Pa·s.[15 16] The LA is the pathway of blood from the PVs to the left ventricle. The purpose of this study was to evaluate and predict the optimal anastomosis size for surgery, meanwhile comparing the results with real-life clinical data to validate the model. Therefore, a pulsatile-state flow can be used to simulate this function. The velocity of blood flow at the PVs is defined as the boundary condition at the inlet. The time-dependent flow velocities were derived from echocardiogram measurements of four PVs in pulsatile-state flow.[17] Our data of time-dependent flow velocities derived from the echo-cardiogram which shows in supplementary file (online supplemental figure 1). In addition, the mitral valve orifice was defined as the outlet, with time-dependent left atrial pressure set as the boundary condition using a trigonometric equation. The equation, as followed, representing normal physiological pressure
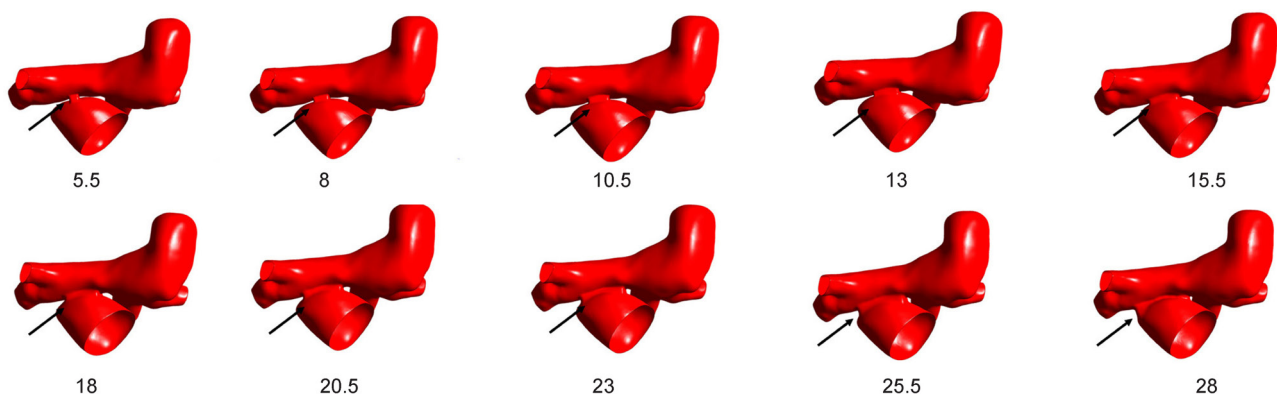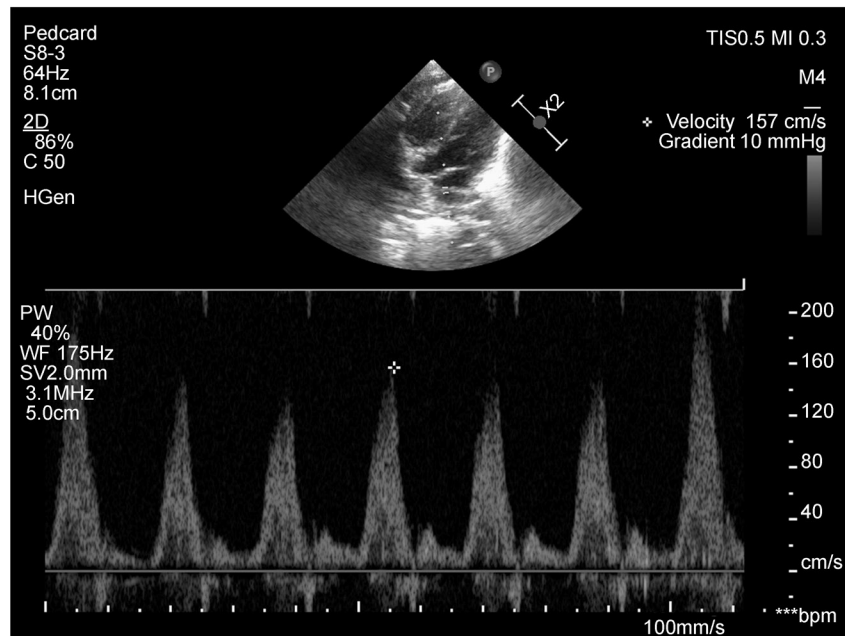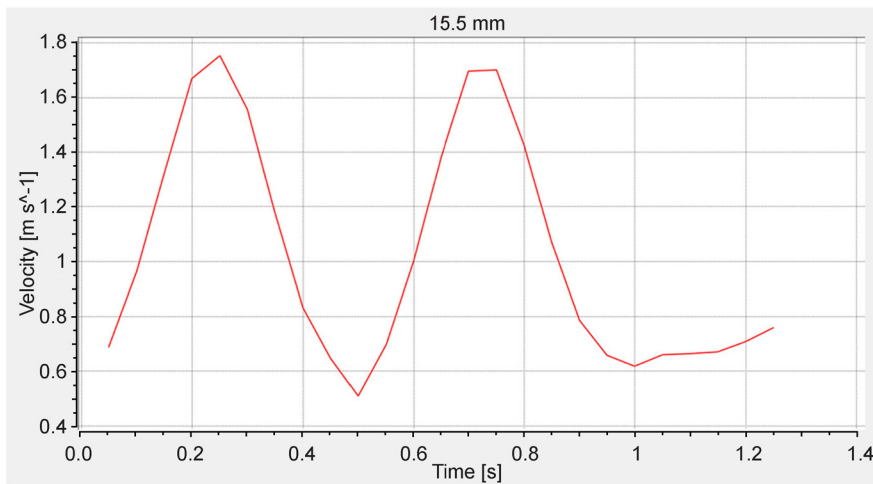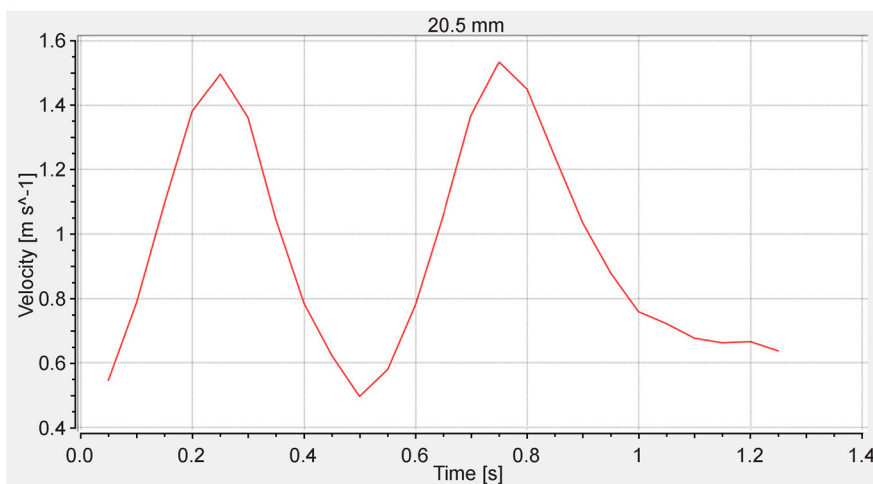

Figure 2 10 models with increment size of anastomosis (mm).

Figure 3 Comparison of Doppler echocardiogram signals and computational fluid dynamics (CFD) velocity plots at anastomosis. (A) Doppler echocardiogram signal at the total anomalous pulmonary venous connection anastomosis, demonstrating the real-time blood flow velocity. (B) CFD-derived blood flow velocity curve for a 15.5 mm anastomosis size, plotted at the simulative anastomosis. (C) CFD-derived blood flow velocity curve for a 20.5 mm anastomosis size, plotted at the simulative anastomosis.

ranging from 4 to 12 mm Hg, as typically observed in healthy individuals.[18]

$$p(t) = 4 \cdot \boldsymbol{a} + 4 \cdot \boldsymbol{a} \left(\sin\left(\frac{2\pi t}{60/f} + 1.5\pi \right) + 1 \right) \qquad (1)$$

where p is the left atrial pressure, t is the latest time at each time step, f is the heart rate, and $\boldsymbol{a}=133$ is the transformation constant of mm Hg to Pa.

In clinical surgery, vertical veins are usually ligated. Therefore, they are neither the entrance nor the outlet of the computational fluid model.

Computational simulation and calculation

Based on the aforementioned models and boundary conditions, the flow field was computed using Fluent (Ansys, USA). Analysis type was set to transient state. In the solver control panel, the advection scheme was set to high resolution, and the maximum number of iteration steps was 20, with a time step of 0.05 s. Furthermore, the residual tolerance was set to 1.0^{e-6} to ensure the calculated results were within an acceptable range. The velocity of blood flow and the area of four PVs were set as inlets.

In clinical practice, the patients underwent surgical repair with an anastomosis size of 20 mm. We obtained the blood flow velocity passing the anastomosis using echocardiography after surgery. This value was compared with the calculated pulsatile-state results.

Energy loss is an important indicator in the evaluation of hemodynamic performance. In this study, energy loss was calculated through power loss and power conversion efficiency.[19 20]

The power loss was defined as:

$$W = Q\left(P + \tfrac{1}{2}\rho v^2\right) \qquad (2)$$

$$W_l = \sum W_{in} - \sum W_{out} \qquad (3)$$

where W, Q, P, ρ, and v represent the power, mass flow, pressure, blood density, and blood velocity, respectively. W_l is the power loss, with $\sum W_{in}$ and $\sum W_{out}$ representing the total power at the inlet and outlet, respectively.

In this study, we calculate the WSS, pressure distribution, and power loss using time-averaged methods.

RESULTS

Hemodynamic parameters such as blood flow velocity, WSS, pressure distribution, and power loss were obtained.

As the anastomotic size increased, the blood flow velocity maps, as shown in online supplemental figure 2, clearly illustrated the streamlines for the 10 models. The regions with higher blood flow velocity were consistently located near the PV–LA anastomosis, with smaller anastomoses resulting in higher velocities.

Figure 3 displayed the actual postoperative blood flow velocity measured by Doppler ultrasound. It also showed the time-related velocity graphs across the PV–LA anastomosis. These graphs depicted the time-variant blood flow velocities calculated by transient CFD simulations, which

were then compared with postoperative Doppler data. The comparison revealed that when the anastomotic size was around 15–20 mm, the actual velocities matched well with the simulated velocities.

WSS is a crucial parameter in hemodynamic analysis and is associated with vascular remodeling. The WSS distribution maps, shown in online supplemental figure 3, indicated that the highest WSS regions were near the anastomosis in all models, with smaller anastomoses exhibiting higher WSS.

The pressure distribution contour of 10 models obtained from CFD analysis is shown in online supplemental figure 4. The pressure on the walls of smaller anastomoses was higher compared with larger anastomosis. High-pressure areas were mainly around the CVs and PVs. Conversely, in the model with larger anastomoses, the pressures in the CV and PV were almost the same as that in the LA.

Power loss visually reflects the work of blood flow and is important in evaluating the expected therapeutic effects of different surgical procedures for TAPVC. The results of power loss and power conversion efficiency of 10 models are presented in table 1. As the size of the anastomosis gradually increases, the pressure in the PVs decreased accordingly, leading to reduced energy loss. However, when the size of the anastomosis exceeded 18 mm, the energy conversion efficiency no longer improved further.

DISCUSSION

It is well known that the size of the anastomosis plays a crucial role in the surgical management of TAPVC. Surgeons are typically encouraged to make the anastomosis as large as possible.[1 5 6] For patients with supracardiac and infracardiac TAPVC, the anastomosis is the only passage for PV blood to reenter the LA after surgery for supracardiac and infracardiac TAPVC patients. However, determining the optimal size of the anastomosis among TAPVC patients remains unclear, and there are few studies focusing on this issue. Jin et al.[21] previously reported a numerical model for TAPVC surgery using a fluid–structure interaction model. They designed simulated anastomoses to compare with actual anastomosis after surgery, but did not compare various sizes of anastomoses within a single case. Other studies have explored numerical models for arteriovenous fistula,[22 23] which involve an anastomosis between an artery and vein. Van Canneyt et al. found that larger anastomoses resulted in lower pressure drops and higher proximal arterial inflow.[22] In our model, the mass of blood flow was the same across all models. Therefore, blood flows more slowly through larger anastomoses and venous confluences, whereas the same volume of blood needs to rush out from smaller anastomoses and venous confluence.

Several studies have reported the risk factors for PVO,[3 24 25] but these studies mainly focus on clinical measurements, such as age, weight, cardiopulmonary bypass time, and the type of TAPVC, rather than the size

Table 1 Power loss comparison between different models

Size of anastomosis	Winlet (mW)	Woutlet (mW)	WI (mW)	E
5.5	106.89	55.71	51.18	0.52
8	65.11	45.30	19.81	0.70
10.5	50.98	43.80	7.18	0.86
13	45.99	42.14	3.84	0.92
15.5	41.67	39.95	1.72	0.96
18	39.97	39.23	0.74	0.98
20.5	39.17	38.33	0.84	0.98
23	38.33	37.71	0.62	0.98
25.5	37.19	36.71	0.49	0.98
28	37.17	36.49	0.68	0.98

E, power conversion rate; Winlet, power of inlet; WI, power loss; Woutlet, power of outlet.

of pulmonary anastomosis. Our study shows that this measurement significantly impacts the simulated results.

Emerging evidence suggests a significant correlation between WSS and the risk of PV stenosis, which is a concerning complication of TAPVC repair. One study highlighted the potential clinical relevance of WSS thresholds.[26] In our analysis, we observed a wide range of WSS values across different anastomosis sizes, with specific patterns indicating how anastomosis shape might impact WSS and subsequent clinical outcomes. These observations support the premise that lower WSS values may reduce the risk of stenosis, advocating for careful consideration of anastomosis geometry in surgical planning to optimize flow dynamics and mitigate adverse outcomes.

In our models, the PVs and LA were assumed to be rigid walls, and the interaction between blood flow and the wall was not considered, which may have influenced the calculated results. Future works should consider using fluid–solid coupling methods to better simulate the treatment of TAPVC in different surgical procedures. Due to lack of precise measurements of anastomoses during surgery and the complexities in designing prospective research, there are ethical concerns in designing small anastomoses for patients with TAPVC. Therefore, our study solely focused on the analysis of a singular case.

In conclusion, the models in this study can determine the optimal size of anastomosis, which is necessary to achieve favorable results, and have significant potential to guide surgical treatment in clinical practice.

ORCID iDs
Jie Jin http://orcid.org/0000-0002-7116-0322
Jing Yu http://orcid.org/0000-0002-0078-4699

REFERENCES
1 Vanderlaan RD, Caldarone CA. Surgical Approaches to Total Anomalous Pulmonary Venous Connection. *Semin Thorac Cardiovasc Surg Pediatr Card Surg Annu* 2018;21:83–91.
2 Hancock Friesen CL, Zurakowski D, Thiagarajan RR, *et al*. Total anomalous pulmonary venous connection: an analysis of current management strategies in a single institution. *Ann Thorac Surg* 2005;79:596–606.
3 Ricci M, Elliott M, Cohen GA, *et al*. Management of pulmonary venous obstruction after correction of TAPVC: risk factors for adverse outcome. *Eur J Cardiothorac Surg* 2003;24:28–36.
4 Hyde JA, Stümper O, Barth MJ, *et al*. Total anomalous pulmonary venous connection: outcome of surgical correction and management of recurrent venous obstruction. *Eur J Cardiothorac Surg* 1999;15:735–40.
5 Behrendt DM, Aberdeen E, Waterson DJ, *et al*. Total Anomalous Pulmonary Venous Drainage in Infants. *Circulation* 1972;46:347–56.
6 Tucker BL, Lindesmith GG, Stiles QR, *et al*. The superior approach for correction of the supracardiac type of total anomalous pulmonary venous return. *Ann Thorac Surg* 1976;22:374–7.
7 Dahl SK, Vierendeels J, Degroote J, *et al*. FSI simulation of asymmetric mitral valve dynamics during diastolic filling. *Comput Methods Biomech Biomed Engin* 2012;15:121–30.
8 Nguyen VT, Wibowo SN, Leow YA, *et al*. A Patient-Specific Computational Fluid Dynamic Model for Hemodynamic Analysis of Left Ventricle Diastolic Dysfunctions. *Cardiovasc Eng Technol* 2015;6:412–29.
9 Wald S, Liberzon A, Avrahami I. A numerical study of the hemodynamic effect of the aortic valve on coronary flow. *Biomech Model Mechanobiol* 2018;17:319–38.

10 van Bakel TMJ, Lau KD, Hirsch-Romano J, *et al*. Patient-Specific Modeling of Hemodynamics: Supporting Surgical Planning in a Fontan Circulation Correction. *J Cardiovasc Transl Res* 2018;11:145–55.

11 Qian Y, Liu JL, Itatani K, *et al*. Computational hemodynamic analysis in congenital heart disease: simulation of the Norwood procedure. *Ann Biomed Eng* 2010;38:2302–13.

12 Loke YH, Capuano F, Balaras E, *et al*. Computational Modeling of Right Ventricular Motion and Intracardiac Flow in Repaired Tetralogy of Fallot. *Cardiovasc Eng Technol* 2022;13:41–54.

13 Cheng Y, Qiao A, Yang Y, *et al*. Numerical Simulation of Hemodynamics in Two Models for Total Anomalous Pulmonary Venous Connection Surgery. *Front Physiol* 2020;11:206.

14 Kim Y-H, Marom EM, Herndon JE II, *et al*. Pulmonary Vein Diameter, Cross-sectional Area, and Shape: CT Analysis. *Radiology* 2005;235:43–9.

15 Lantz J, Henriksson L, Persson A, *et al*. Patient-Specific Simulation of Cardiac Blood Flow From High-Resolution Computed Tomography. *J Biomech Eng* 2016;138.

16 Ding J, Liu Y, Wang F. Influence of bypass angles on extracardiac Fontan connections: a numerical study. *Int J Numer Method Biomed Eng* 2013;29:351–62.

17 Lantz J, Gupta V, Henriksson L, *et al*. Impact of Pulmonary Venous Inflow on Cardiac Flow Simulations: Comparison with In Vivo 4D Flow MRI. *Ann Biomed Eng* 2019;47:413–24.

18 Figueras-Coll M, Sanchez-de-Toledo J, Gran F, *et al*. Echocardiography in the Assessment of Left Atrial Pressure After Pediatric Heart Surgery. *World J Pediatr Congenit Heart Surg* 2015;6:438–42.

19 Guadagni G, Bove EL, Migliavacca F, *et al*. Effects of pulmonary afterload on the hemodynamics after the hemi-Fontan procedure. *Medical Engineering & Physics* 2001;23:293–8.

20 Migliavacca F, Dubini G, Bove EL, *et al*. Computational fluid dynamics simulations in realistic 3-D geometries of the total cavopulmonary anastomosis: the influence of the inferior caval anastomosis. *J Biomech Eng* 2003;125:805–13.

21 Jin J, Ma X, Fu X, *et al*. Fluid-Structure Interaction Model for Predicting Surgical Result of Total Anomalous Pulmonary Venous Connection and Estimating Pulmonary Venous Properties. *Cardiovasc Eng Technol* 2022;13:725–34.

22 Van Canneyt K, Pourchez T, Eloot S, *et al*. Hemodynamic impact of anastomosis size and angle in side-to-end arteriovenous fistulae: a computer analysis. *J Vasc Access* 2010;11:52–8.

23 Kharboutly Z, Fenech M, Treutenaere JM, *et al*. Investigations into the relationship between hemodynamics and vascular alterations in an established arteriovenous fistula. *Med Eng Phys* 2007;29:999–1007.

24 Shi G, Zhu Z, Chen J, *et al*. Total Anomalous Pulmonary Venous Connection: The Current Management Strategies in a Pediatric Cohort of 768 Patients. *Circulation* 2017;135:48–58.

25 Karamlou T, Gurofsky R, Al Sukhni E, *et al*. Factors associated with mortality and reoperation in 377 children with total anomalous pulmonary venous connection. *Circulation* 2007;115:1591–8.

26 Hammer PE, McEnaney K, Callahan R, *et al*. The Role of Elevated Wall Shear Stress in Progression of Pulmonary Vein Stenosis: Evidence from Two Case Studies. *Children (Basel)* 2021;8:729.